Journal of Engineering Physics and Thermophysics, Vol. 73, No. 5, 2000

PARAMETERS OF SUPERDEEP PENETRATION OF A COPPER POWDER INTO STEEL

O. V. Roman, S. K. Andilevko, S. S. Karpenko, and G. P. Okatova

UDC 534.2

The results of a series of experiments on superdeep penetration of copper-powder particles into a steel target are presented. The main parameters of the process and its efficiency are determined on the basis of statistical processing of the data on sequential breakdown of foil layers that are placed in the target perpendicular to the direction of motion of the penetrating particles.

Experimental investigation of the process of superdeep penetration [1, 2] from the moment of its detection till now has been hindered by the conditions under which this phenomenon is realized. Direct visualization of the process of penetration is impossible, first, because for it to originate one must use explosion schemes which give many fragments but do not allow the use of sensitive recording pulsed equipment. Second, a layer-by-layer chemical analysis of the treated specimens for determination of the excess of the level of the introduced material over the background one turned out to be inefficient, because this excess is, as a rule, very small [3]. There exist methods of direct visualization of the channels and the penetrated particles [4]; however, due to the smallness of the introduced objects ($D < 100$ μm) this method makes it impossible to form an idea about the phenomenon as a whole. The present paper gives a technique for processing the results of a series of experiments with loading of a steel obstacle by the flux of a copper powder of narrow fraction ($D_0 \approx 55$ μm) which, in the authors' opinion, allows one to solve this problem successfully.

To realize the effect of superdeep penetration, we used the scheme of acceleration of a copper-powder flux (Fig. 1a), which is standard for many works in this field [1-5] and which makes it possible to treat the tested specimen with a gas-powder jet with an average density of 2000–4000 kg/m^3 at a mean velocity of 1–2 km/sec. The total mass of the launched copper powder with $D_0 \approx 55$ μm is equal to about 0.204 kg with a density of the filling of 5101 kg/m^3. The launched jet gets on the upper surface of the tested combined specimen (CS) (Fig. 1b) and produces conditions necessary for the realization of the effect of superdeep penetration (SDP). The results of it can be evaluated by analyzing the sequential breakdown of foil layers that are placed in the CS chamber perpendicular to the direction of launching. It is known with certainty [5, 6] that the introduction of a large number of interfaces hinders the realization of the process of superdeep penetration due to multiple disintegration of discontinuity, which substantially weakens the shock loading of the foil in the CS chamber. To weaken the shock loading even greater and to prevent sticking of the foil layers during the treatment, thin layers of tracing paper are additionally laid between them. The results of the treatment are analyzed by counting the number of particles on the foil layers by a light microscope with ×500–1000 magnification. In this case, using the attachment for a stereological analysis of the image, we determine the size of the revealed inclusions; this allows one to judge the total mass of the penetrating material. A typical form of copper particles on the aluminum foil is given in Fig. 2a and b. The choice of the penetration material (copper) and foil-detector (aluminum, the thickness is $T = 10$ μm) is determined by the desire to obtain additional advantages in detection of particles due to the color difference (the reddish shade of copper is in good contrast with silver aluminum). In this case, it was taken into account that plastic copper will not be crushed in collision with the obstacle, because the crushing could lead to a certain violation of the integrity of the perception of the experi-

Scientific-Research Institute of Pulsed Processes of the Belarusian State Science and Production Concern of Powder Metallurgy, Minsk, Belarus. Translated from Inzhenerno-Fizicheskki Zhurnal, Vol. 73, No. 5, pp. 1056-1063, September–October, 2000. Original article submitted December 24, 1999.

1062-0125/00/7305-1033$25.00

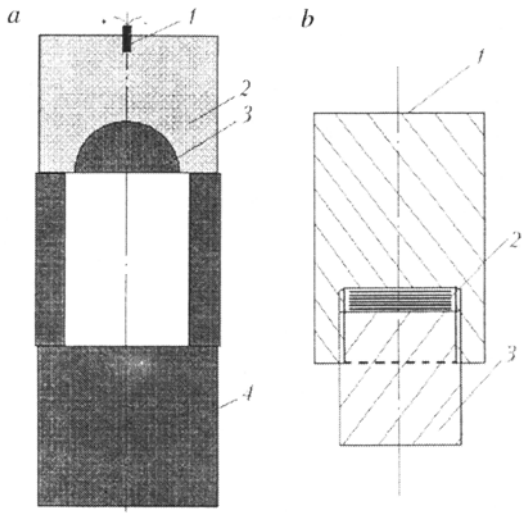

Fig. 1. Schematic diagrams of loading (a): [1) initiator; 2) explosive charge; 3) launched powder; 4) specimen] and a combined specimen (b): [1) frontal part; 2) foil layers; 3) shutting plug].

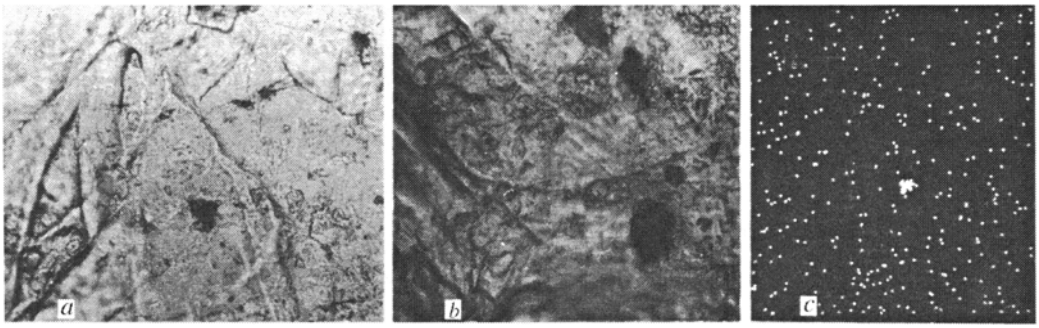

Fig. 2. Typical form of detected inclusions on the 1st (a) and 8th (b) foil layer (L = 35 mm) and analysis of the amount of copper on the foil surface (c).

ment. The result of a microchemical analysis made on a Nanolab-7 scanning electron microscope where the local peak of copper concentration on the foil surface falls precisely on the inclusion can serve as a confirmation of the fact that it is the copper inclusions that are registered on the foil (Fig. 2b). A total of 10 layers of foil were used in one laying, inclusions for each CS were counted on each layer, and the counted area was 12.28 mm^2 with the total area of each layer of foil being ~707 mm^2.

A statistical analysis of the breakdown of foil layers allows one to obtain rather extensive information on the parameters of penetration. The most important factor is undeniably the number of particles recorded on the foil. Let the numbering of layers denoted by the subscript i begin from the rear surface of the obstacle and change from 1 to n (in our particular case, n = 10). The number of particles on each layer of foil is N_i, and the mean size of the recorded inclusions is D_i. The total number of particles per square millimeter which have broken the tested CS layer is

$$N = \frac{1}{nS_f} \sum_{i=1}^{n} N_i , \tag{1}$$

where S_f is the area of the foil on which the particles were counted. The mean diameter of the detected inclusions is

$$\overline{D} = \frac{1}{n} \sum_{i=1}^{n} D_i . \tag{2}$$

The velocity of the particle V_r after the breakdown of the foil with a thickness T [7] (we assume the particle to be spherical and nondeformable and the angle of its incidence onto the foil to be normal) is

$$V_r = \begin{cases} 0, & 0 \le V_0 \le V, \\ a\,(V_0^p - V^p)^{\frac{1}{p}}, & V_0 > V, \end{cases} \tag{3}$$

where V_0 is the velocity of the individual striker before collision with the foil,

$$V = \beta \sqrt{\left(f(z) \left(\frac{D^3}{M} \right) \right)} = \frac{\beta}{\sqrt{\rho_p}} \sqrt{\left(\frac{6}{\pi} f(z) \right)},$$

$$a = \frac{M}{M + \frac{M_t}{3}}, \quad M = \rho_p \frac{\pi}{6} D^3,$$

$$p = 2 + \frac{z}{3}, \quad M_t = \rho_f \pi D^3 \frac{z}{4}, \tag{4}$$

$$f(z) = z + \exp(-z) - 1, \quad z = \frac{T}{D},$$

ρ_f and ρ_p is the density of the foil and the particle, respectively, and β is the material constant. In this case the velocity of particles U_i that are detected on the i-th layer at the instant of its entry into the chamber with the foil is

$$\delta_i \frac{\left(\sum_{k=0}^{i-2} a^{kp} \right)^{\frac{1}{p}}}{a^{i-2}} V < U_i \le \frac{\left(\sum_{k=0}^{i-1} a^{kp} \right)^{\frac{1}{p}}}{a^{i-1}} V, \quad \delta_i = \begin{cases} 0, & i = 1, \\ 1, & i \ne 1. \end{cases} \tag{5}$$

Using (5), we can determine the ranges of particle velocities depending on the number of the foil (β = 1750 $m^{5/2}/(sec \cdot kg^{1/2})$ for aluminum [7], ρ_p = 8900 kg/m^3, and ρ_f = 2710 kg/m^3). Assuming that the velocity of the particle detected on the i-th layer can, with equal probability, take on any value from the corresponding range and introducing for each layer the mean velocity

$$u_i = \frac{V}{2a^{i-2}} \left[\delta_i \left(\sum_{k=0}^{i-2} a^{kp} \right)^{\frac{1}{p}} + \left(\sum_{k=0}^{i-1} a^{kp-1} \right)^{\frac{1}{p}} \right], \tag{6}$$

we determine the residual energy of the penetrating particle flux as

$$E_r = \frac{M}{2} \sum_{i=1}^{n} N_i u_i^2 = \frac{MV^2}{8} \sum_{i=1}^{n} \frac{N_i}{a^{2(i-1)}} \left[\delta_i \left(\sum_{k=0}^{i-2} a^{kp} \right)^{\frac{1}{p}} + \left(\sum_{k=0}^{i-1} a^{kp-1} \right)^{\frac{1}{p}} \right]^2. \tag{7}$$

TABLE 1. Data on Counting the Number of Inclusions Detected on Different Layers of Foil

L, mm	N_1	N_2	N_3	N_4	N_5	N_6	N_7	N_8	N_9	N_{10}
35	19	77	375	133	127	98	50	36	70	30
40	25	49	52	22	67	31	43	65	14	15
50	27	21	31	84	25	18	20	20	24	12

TABLE 2. Results of Statistical Processing of Data

No. of specimen	$\bar{d}$, μm	U_{min}, m/sec	U_{max}, m/sec	Fraction, mm
		$L = 35$ mm		
1	2.1	0	98	1.9
2	2.2	95	164	7.7
3	2.0	182	320	36.9
4	3.2	173	257	13.2
5	2.5	373	603	12.5
6	3.2	381	561	9.6
7	2.3	1198	1991	4.8
8	10.3	134	157	3.6
9	5.1	434	564	6.9
10	2.9	2449	3795	2.9
		$L = 40$ mm		
1	5.4	0	50	6.5
2	2.7	83	136	12.8
3	3.5	107	158	13.6
4	3.6	153	220	5.7
5	3.6	220	314	17.5
6	3.7	302	426	8.2
7	4.1	357	490	11.2
8	3.8	570	798	17.0
9	3.3	1129	1650	3.6
10	3.2	1807	2666	3.9
		$L = 50$ mm		
1	7.1	0	41	10.0
2	5.3	51	77	7.7
3	3.8	100	145	11.6
4	4.7	119	161	30.9
5	3.8	205	290	9.5
6	3.3	361	528	6.9
7	4.6	298	397	7.7
8	3.7	602	850	8.9
9	4.2	638	870	2.9
10	2.7	3099	4846	3.9

This technique allows a quantitative comparison of the efficiency of superdeep penetration for different schemes of loading and at different depths. To illustrate this fact, we subjected steel CSs with different thicknesses of the frontal part L to loading. The data on counting the number of particles for three cases are given in Table 1, and the results of their statistical processing for three lengths of the tested specimens are presented in Table 2. Figure 3 illustrates the velocity distribution of the penetrated particles in the form of the corresponding nomograms. The mean velocity is 413.3, 416.8, and 349.1 m/sec for L = 35, 40, and 50 mm, respec-

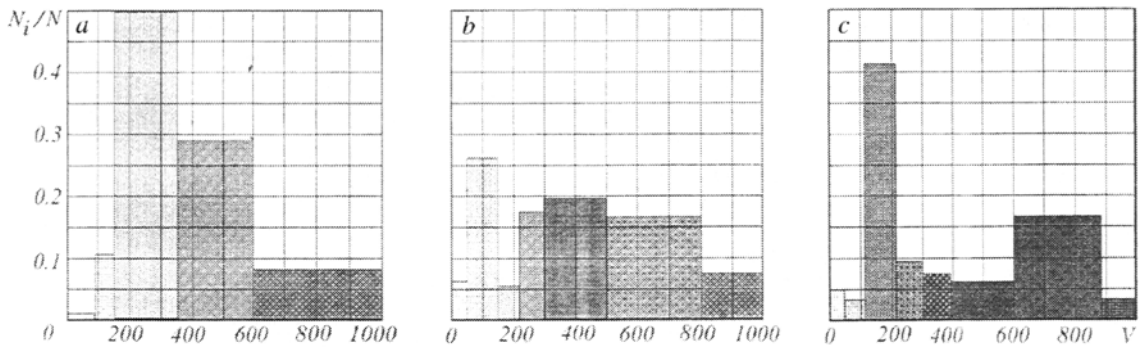

Fig. 3. Nomograms of the velocity distribution in the particle flux for L = 35 (a), 40 (b), and 50 mm (c). V, m/sec.

tively, and the number of recorded inclusions per unit area is 83, 31, and 22 mm^{-2} (in the same sequence). The mean residual energy was determined as $8.81 \cdot 10^{-6}$ J for L = 35 mm, $7.85 \cdot 10^{-6}$ J for L = 40 mm, and $7.00 \cdot 10^{-6}$ J for L = 50 mm. The presented data make it possible to construct the dependence of the number of penetrated particles N, their mean diameter D, and the mean residual energy E_r on the depth of penetration L (Fig. 4a, b, and c). The datum point corresponding to the number of particles on the surface of the obstacle can be assigned if we count the limiting number of inclusions per unit area; in our case it is 1383 mm^{-2}. The beginning ($0 \le L \le 35$ mm) of the empirical relation (the solid curve) is shown in Fig. 4a and b by a straight line, since data on the behavior of the presented quantities within this range are absent now. One can note a fast decrease in the number of introduced particles and the residual energy of the flux with increase in the depth; at the same time, the mean diameter of the particles, which quickly decreases to L = 35 mm, then begins to increase slowly. This latter result is attributable to the probable effect of two factors: 1) in penetration, the conditions under which the loss of particle mass can be altered by the process of "sticking" can be realized; 2) the number of very large inclusions which affect the mean diameter of detected particles decreases with increase in the depth much more slowly than the number of small inclusions (the latter are most likely "worked out" during the motion). Thus, if for the total number of particles penetrated to depths L = 35, 40, and 50 mm their relative number can be determined as 3.77, 1.41, and 1, respectively (the number of particles for L = 50 mm was taken to be unity), then for large inclusions this dynamics turns out to be different: 1.51, 1.02, and 1 (the total number of large objects that exceed in diameter the largest mean size 4.5 μm is 98, 66, and 65 particles per 12.28 mm^2 for L = 35, 40, and 50 mm, respectively). The effect of the large particles on the mean diameter under these conditions will, undoubtedly, substantially increase, which will lead to an increase in the mean size with increase in L.

The dependences of the change in the number of particles and their size on the depth (Fig. 4a and b) can be approximated by analytical functions

$$N(L) = N_0 \exp(-\eta L^b) \tag{8}$$

and

$$D(L) = 2.8 + g\,|L - 35|^{\sigma}\ \mu\text{m}, \tag{9}$$

where $\eta \approx 0.035$, $b \approx 1.24$, $g \approx 0.0000042$ μm, and $\sigma \approx 4.6$. This makes it possible to calculate the concentration of the introduced substance

$$c(L) = \frac{dM(L)}{\rho_t S dL}, \tag{10}$$

here $M(L)$ and S are the mass of the flux and the area of the treated section, ρ_t is the density of the target;

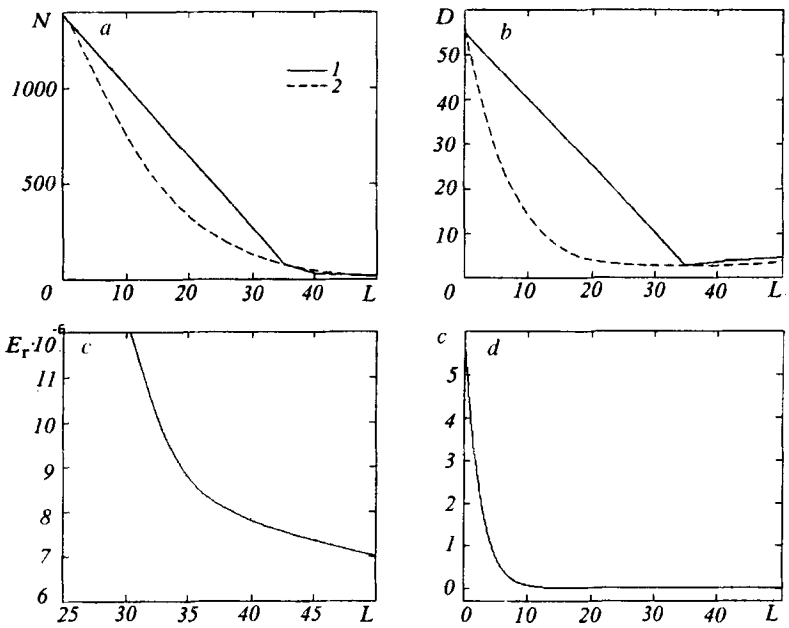

Fig. 4. Dependences $N(L)$ (a), $D(L)$ (b), $E_r(L)$ (c), and $c(L)$ (d): 1) experimental data; 2) approximation. $N(L)$, mm^{-2}; $D(L)$, μm; $E_r(L)$, J; $c(L)$, %; L, mm

$$M(L)=\frac{\pi}{6}\rho_p D^3(L)N(L), \tag{11}$$

consequently,

$$c(L)=-\frac{\pi}{2}\frac{\rho_p}{\rho_t}\frac{D^2(L)N(L)}{S}\left(\frac{d}{dL}D(L)+\frac{D(L)}{3N(L)}\frac{d}{dL}N(L)\right). \tag{12}$$

When $D(L)$ is not a monotonically decreasing function of L, formula (12) must be corrected. Indeed, on those portions where $d(D(L))/dL$ is nonnegative, one should not expect precipitation of the particle material on the "walls" of the channel and it can be introduced only by stopping the fraction of the flux particles in the layer dL. Instead of (12) we obtain the equation

$$c(L)=-\frac{\pi}{2}\frac{\rho_p}{\rho_t}\frac{D^2(L)N(L)}{S}\left(\delta\left(\frac{d}{dL}D(L)\right)\frac{d}{dL}D(L)+\frac{D(L)}{3N(L)}\frac{d}{dL}N(L)\right), \tag{13}$$

where

$$\delta\left(\frac{d}{dL}D(L)\right)=\begin{cases}1, & \frac{d}{dL}D(L)\le 0,\\ 0, & \frac{d}{dL}D(L)>0.\end{cases} \tag{14}$$

Figure 4d shows results of calculating the concentration of the introduced copper as a function of the obstacle depth. We note that near the surface the level of concentration can reach several percent by mass, whereas for the reference points of the discussed experiment we obtained the following values: $c(35) \approx 0.00001038\%$, $c(40) \approx 0.000006431\%$, and $c(50) \approx 0.000006075\%$. This result is in agreement with the data of [8]. The total amount of material introduced into the obstacle is

$$M_{ins} = \rho_t S \int_{L_0}^{L_{max}} c(L)\, dL, \tag{15}$$

where L_0 and L_{max} are the initial and final depths, respectively. In our case, the first is zero and the second is 0.05 m; the total mass of the introduced powder is $M_{ins} \approx$ 0.0007961 kg, which accounts for 0.39% of the whole material launched. As a matter of convention, however, the first 5 mm of the treated material are not considered in SDP analysis (indeed, 55-μm particles can reach a depth of 5 mm under favorable conditions and beyond the SDP). Therefore, the effective mass of the penetrated material turns out to be much smaller (L_0 = 0.005 m): $M_{ins} \approx 8.535 \cdot 10^{-5}$ kg, i.e., about 0.04% of the initial mass of the powder. The latter quantity can be considered as the efficiency of the scheme by the mass of the introduced material.

Thus, during the series of experiments on the superdeep penetration of a copper powder into a steel obstacle we succeeded in finding the basic parameters of superdeep penetration (mass of the introduced material, distribution of concentration over the depth of the obstacle, number of penetrating particles as a function of depth, etc.). The velocity and energy characteristics of the process are determined. The fact that residual mean velocities of the flux for L = 35 and 40 mm virtually coincide makes it possible to indirectly confirm the conclusions [5, 6] that the penetration occurs at a certain stationary velocity whose magnitude depends on the character of the obstacle loading more than on the parameters of the particles. The above experimental technique was given the name technique of a combined specimen (TCS).

The authors are thankful to V. A. Shilkin for useful advice and help in the experiments.

This work was carried out within the framework of a grant from the Fund for Fundamental Research of the Republic of Belarus (T98-199).

NOTATION

D, particle diameter; N, number of particles; S, area; n, number of foil layers; T, foil thickness; V, minimum velocity of the particle necessary for the breakdown of a single foil; U, velocity; a, p, z, $f(z)$, β, and M_t, local notation explained in the text; L, depth (thickness of the frontal part of the specimen); b, g, σ, and η coefficients of approximation; M, mass; u, mean velocity; c, concentration of the introduced material; δ, function; ρ, density. Subscripts: 0, initial value; i, number of foil; f, foil; k, summation; p, particle; t, target; ins, introduced material; r, residual values; max, final depth.

REFERENCES

1. V. G. Gorobtsov, S. M. Usherenko, and V. Ya. Furs, *Poroshk. Metall.*, No. 3, 8-12 (1979).
2. S. K. Andilevko, O. V. Roman, V. G. Gorobtsov, and S. M. Usherenko, *Poroshk. Metall.*, No. 3, 100-102 (1987).
3. S. K. Andilevko, O. V. Roman, V. A. Shilkin, V. Slobodsky, and S. M. Usherenko, in: L. M. Murr, K. P. Staudhammer, and M. A. Meyers (eds.), *Metallurgical and Material Application of Shock-Wave and High-Strain-Rate Phenomena* (1995), pp. 437-443.
4. S. K. Andilevko, E. A. Doroshkevich, V. A. Shilkin, and S. M. Usherenko, *Int. J. Heat Mass Transfer*, **41**, Nos. 6-7, 951-956 (1998).
5. L. V. Al'tshuler, S. K. Andilevko, G. S. Romanov, and S. M. Usherenko, *Inzh.-Fiz. Zh.*, **61**, No. 1, 41-45 (1991).
6. S. K. Andilevko, *Superdeep Mass Transfer of Discrete Microparticles in Metal Obstacles under the Conditions of Loading of the Latter by a Powder Flux*, Candidate's Dissertation in Physics and Mathematics, Minsk (1991).
7. J. Zukas, in: *Dynamics of Shock* [Russian translation], Moscow (1986), pp. 116-168.
8. S. K. Andilevko, S. M. Usherenko, and V. A. Shilkin, *Pis'ma Zh. Tekh. Fiz.*, **24**, No. 17, 19-21 (1998).